

An Extreme Value Bayesian Lasso for the Conditional Bulk and Tail

M. DE CARVALHO[†], S. PEREIRA[‡], P. PEREIRA^{*}, and P. DE ZEA BERMUDEZ[‡]

[†]*School of Mathematics, University of Edinburgh, UK (miguel.decarvalho@ed.ac.uk)*

[‡]*Faculdade de Ciências and CEAUL, Universidade de Lisboa, Portugal (sapereira@fc.ul.pt)*

^{*}*ESTSetúbal/IPS and CEAUL, Portugal (paula.pereira@estsetubal.ips.pt)*

Abstract

We introduce a novel regression model for the conditional bulk and conditional tail of a possibly heavy-tailed response. The proposed model can be used to learn the effect of covariates on an extreme value setting via a Lasso-type specification based on a Lagrangian restriction. Our model can be used to track if some covariates are significant for the bulk, but not for the tail—and vice-versa; in addition to this, the proposed model bypasses the need for conditional threshold selection in an extreme value theory framework. We assess the finite-sample performance of the proposed methods through a simulation study that reveals that our method recovers the true conditional distribution over a variety of simulation scenarios, along with being accurate on variable selection. Rainfall data are used to showcase how the proposed method can learn to distinguish between key drivers of moderate rainfall, against those of extreme rainfall.

KEY WORDS: Conditional bulk and tail; Extended Generalized Pareto distribution; Heavy-tailed response; Lasso; L1-Penalization; Nonstationary extremes; Statistics of extremes; Variable selection.

1 INTRODUCTION

Learning about what are the drivers of risk is key to a variety of fields, including climatology, environmental sciences, finance, forestry, and hydrology. Mainstream approaches for learning about such drivers or predictors of risk include, for instance, Davison and Smith (1990),

Chavez-Demoulin and Davison (2005), Eastoe and Tawn (2009), Wang and Tsai (2009), Chavez-Demoulin et al. (2016), and Huser and Genton (2016).

A main contribution of this paper rests on a Bayesian regression model for the conditional bulk and conditional tail of a possibly heavy-tailed response. Our model pioneers the development of regression methods in an extreme value framework that allow for some covariates to be significant for the bulk but not for the tail (and vice-versa). Some further comments on the proposed model are in order. First, the proposed model bypasses the need for (conditional) threshold selection; such selection is particularly challenging on a regression framework as it entails selecting a function of the covariate (say, $u_{\mathbf{x}}$) rather than a single scalar. Second, our method models both the conditional bulk and the conditional tail; thus, the proposed model offers a full portrait of the conditional distribution, while it is still able to extrapolate beyond observed data into the conditional tail. Finally, our method is directly tailored for variable selection in an extreme value framework; in particular, it can be used to track what covariates are significant for the bulk and tails.

In an extreme value framework, interest focuses on modelling the most extreme observations—disregarding the central part of the distribution. Usually, the effort centers on modelling the tail of the distribution using a generalized extreme value distribution, in a block maxima framework, or by the generalized Pareto distribution, in a peaks over threshold setting (Embrechts et al., 1997; Coles, 2001; Beirlant et al., 2004). Naturally, many observations are disregarded using the latter approaches, and the choice of the block size / or threshold are far from straightforward. Moreover, in many situations of applied interest it would be desirable to model both the bulk of the data along with the extreme values, in a regression framework. Our model builds over Papastathopoulos and Tawn (2013) and Naveau et al. (2016) who proposed an extended generalized Pareto distribution (EGPD) so to model jointly low, moderate and extreme observations—without the need of threshold selection; other interesting options for modeling both the bulk and the tail of a distribution, include extreme value mixture models (e.g. Frigessi et al., 2002; Behrens et al., 2004; Carreau and Bengio, 2009; Cabras and Castellanos, 2011; MacDonald et al., 2011; do Nascimento et al., 2012).

The proposed model can be regarded as a Bayesian Lasso-type model for the bulk and tail of an heavy-tailed response. The Bayesian Lasso was introduced by Park and Casella (2008) as a Bayesian version of the Tibshirani's Lasso (Tibshirani, 1996). Roughly speaking, the

Lasso is a regularization method that is naturally tailored for variable selection, that shrinks some regression coefficients, and sets others to 0; for a recent review of Bayesian regularization methods see Polson and Sokolov (2019). As we clarify below (Section 2.2), our model has also points of contact with quantile regression. Indeed, by modeling both the conditional bulk and the conditional tail, our model bridges quantile regression (Koenker and Bassett, 1978) with extremal quantile regression (Chernozhukov, 2005). Finally, as a byproduct, this paper contributes to the literature on Bayesian inference for Pareto distributions (Arnold and Press, 1989; de Zea Bermudez and Turkman, 2003; Castellanos and Cabras, 2007; de Zea Bermudez and Kotz, 2010; Villa, 2017).

The rest of this paper unfolds as follows. In Section 2 we introduce the proposed methods. Section 3 assesses the performance of the proposed methods, and report the main findings of our numerical studies. A real data illustration is included in Section 4. We conclude in Section 5.

2 EXTREME VALUE BAYESIAN LASSO

To streamline the presentation, the proposed methods are introduced in a step-by-step fashion, with the most flexible version of our model being introduced in Section 2.4.

2.1 THE EXTENDED GENERALIZED PARETO FAMILY

Our starting point for modeling is the so-called extended generalized Pareto distribution (EGPD), as proposed in Papastathopoulos and Tawn (2013) and Naveau et al. (2016). The cumulative distribution function of a EGPD is

$$F(y) = G(H(y)),$$

where H is the generalized Pareto distribution function

$$H(y) = 1 - \left(1 + \frac{\xi y}{\sigma}\right)^{-1/\xi},$$

defined on $\{y \in (0, \infty) : 1 + \xi y / \sigma > 0\}$. Here, $\sigma > 0$ is a scale parameter, $\xi \in \mathbb{R}$ is the shape parameter; the case $\xi = 0$ should be understood by taking the limit $\xi \rightarrow 0$. The shape parameter ξ is known as the extreme value index and it controls the rate of decay of the tail. Following Naveau et al. (2016), we assume that the carrier function G obeys the following conditions:

- A. $\lim_{v \rightarrow 0^+} \frac{1-G(1-v)}{v} = a$, with $a > 0$.
- B. $\lim_{v \rightarrow 0^+} \frac{G\{v w(v)\}}{G(v)} = b$, with $b > 0$ and $w(v) > 0$ being such that $w(v) = 1 + o(v)$ as $v \rightarrow 0^+$.
- C. $\lim_{v \rightarrow 0^+} \frac{G(v)}{v^\kappa} = c$, with $c > 0$.

Assumption A ensures a Pareto-type tail, whereas Assumptions B–C ensure that the bulk is driven by the carrier G . In more detail, Assumption A implies that

$$\lim_{y \rightarrow y_*} \frac{1 - F(y)}{1 - H(y)} = a,$$

and thus it can be understood as a tail-equivalence condition (Embrechts et al., 1997, Section 3.3), where $y^* = \inf\{y : F(y) < 1\}$ is the so-called right endpoint, here assumed to be positive. Since tail-equivalence implies that both F and H are on the same domain of attraction (Resnick, 1971), it follows from Assumption A that ξ can be literally interpreted as the extreme value index of $F(y) = G(H(y))$.

For parsimony reasons we focus on modeling G using a parametric class, so that $G(v) \equiv G_\kappa(v)$, with $\kappa \in \mathbb{R}^q$. The canonical example of a parametric carrier is $G_\kappa(v) = v^\kappa$, with $\kappa > 0$ controlling the shape of the lower tail, with a larger value of κ leading to less mass close to zero; we refer to the EGPD distribution with the latter carrier as the canonical EGPD.

Below, we use the notation $Y \sim \text{EGPD}_G(\kappa, \sigma, \xi)$ to denote that Y follows an EGPD with parameters (κ, σ, ξ) with carrier G ; also, \mathcal{G} will be used to represent the space of all carrier functions $G : (0, \infty) \rightarrow [0, 1]$ obeying Assumptions A, B, and C.

2.2 A FIRST CONDITIONAL MODEL FOR THE BULK AND TAIL OF A POSSIBLY HEAVY-TAILED RESPONSE

The first version of our model considers the following specification for the conditional distribution function,

$$F(y \mid \mathbf{x}) = G_{\kappa(\mathbf{x})}(H(y)), \quad (1)$$

where $\mathbf{x} = (x_1, \dots, x_p) \in \mathbb{R}^p$ is a vector of covariates. Here, $\kappa(\mathbf{x})$ is a vector function with components given by inverse link functions

$$\kappa(\mathbf{x}) = (\kappa_1(\mathbf{x}^\top \boldsymbol{\beta}_1), \dots, \kappa_q(\mathbf{x}^\top \boldsymbol{\beta}_q)), \quad (2)$$

and $G_{\kappa(\mathbf{x})} \in \mathcal{G}$, for every $\mathbf{x} \in \mathcal{X} \subseteq \mathbb{R}^p$; here and below, $\boldsymbol{\beta}_j = (\beta_{1,j}, \dots, \beta_{p,j}) \in \mathbb{R}^p$, for $j = 1, \dots, q$. For reasons that will become evident below, for now we do not allow (σ, ξ) to depend on the covariate \mathbf{x} , but we will extend the specification in (1) to the latter setting in Section 2.4.

Example 1 (Power carrier, exponential link). The canonical embodiment of the first version of our model in (1) is obtained by specifying

$$G_{\kappa(\mathbf{x})}(v) = v^{\kappa(\mathbf{x})}, \quad \kappa(\mathbf{x}) = \exp(\mathbf{x}^T \boldsymbol{\beta}). \quad (3)$$

Example 2 (Beta carrier, exponential link). Another variant of (1) is obtained by specifying

$$G_{\kappa(\mathbf{x})}(v) = 1 - Q_{\kappa(\mathbf{x})}(1 - v^{\kappa(\mathbf{x})}), \quad \kappa(\mathbf{x}) = \exp(\mathbf{x}^T \boldsymbol{\beta}), \quad (4)$$

where

$$Q_{\kappa(\mathbf{x})}(v) = \frac{1 + \kappa(\mathbf{x})}{\kappa(\mathbf{x})} v^{1/\kappa(\mathbf{x})} \left(1 - \frac{v}{1 + \kappa(\mathbf{x})} \right)$$

is the distribution function of a Beta distribution with parameters $(1/\kappa(\mathbf{x}), 2)$.

Example 3 (Power mixture carrier, exponential links). Still another variant of this first version of the model is obtained by specifying

$$G_{\kappa(\mathbf{x})}(v) = \pi v^{\kappa_1(\mathbf{x})} + (1 - \pi) v^{\kappa_2(\mathbf{x})},$$

with $0 < \pi < 1$ and

$$\kappa_1(\mathbf{x}) = \exp(\mathbf{x}^T \boldsymbol{\beta}_1), \quad \kappa_2(\mathbf{x}) = \exp(\mathbf{x}^T \boldsymbol{\beta}_2).$$

The conditions on the intercepts $\beta_{1,1} > \beta_{1,2}$ and $\beta_{j,1} = \beta_{j,2}$, for $j = 2, \dots, q$, leads to $\kappa_1(\mathbf{x}) > \kappa_2(\mathbf{x})$ and is used for identification purposes.

A consequence of (1) is that

$$F^{-1}(p \mid \mathbf{x}) = \begin{cases} \frac{\sigma}{\xi} [\{1 - G_{\kappa(\mathbf{x})}^{-1}(p)\}^{-\xi} - 1], & \xi \neq 0, \\ -\frac{\sigma}{\xi} \log\{1 - G_{\kappa(\mathbf{x})}^{-1}(p)\}, & \xi = 0, \end{cases} \quad (5)$$

where $F^{-1}(p \mid \mathbf{x}) = \inf\{y : F(y \mid \mathbf{x}) \geq p\}$, for $0 < p < 1$. Equation (5) warrants some remarks on links with quantile regression. The first version of our model in (1) can be regarded as a model that bridges quantile regression (Koenker and Bassett, 1978) with extremal quantile

regression (Chernozhukov, 2005), in the sense that it offers a way to model both moderate and high quantiles. Quantile regression (Koenker, 2005) allows for each τ th conditional quantile to have its own slope β_τ , according to the following linear specification

$$F^{-1}(\tau \mid \mathbf{x}) = \mathbf{x}^T \boldsymbol{\beta}_\tau, \quad 0 < \tau < 1. \quad (6)$$

In the same way that high empirical quantiles fail to extrapolate into the tail of a distribution, the standard version of quantile regression in (6) is unable to extrapolate into the tail of the conditional response.

Next, we describe Bayesian Lasso modeling and inference for the first version of our model. For parsimony, below we will focus on the version of the model that sets $q = 1$ in (2), so that $\kappa(\mathbf{x}) = k(\mathbf{x}^T \boldsymbol{\beta})$.

2.3 REGULARIZATION AND BAYESIAN INFERENCE

Let $\{(\mathbf{x}_i, y_i)\}_{i=1}^n$ be a random sample from $F(\mathbf{x}, y)$. We propose a Bayesian Lasso-type specification for the model in (1) so to regularize the log-likelihood. Specifically, let $G_{\kappa(\mathbf{x})} \in \mathcal{G}$, with $\kappa(\mathbf{x})$ being a function of \mathbf{x} , so that the likelihood becomes

$$L(\boldsymbol{\beta}, \sigma, \xi) = \prod_{i=1}^n h(y_i) g_{\kappa(\mathbf{x}_i)}(H(y_i)),$$

where $\boldsymbol{\beta} = (\beta_1, \dots, \beta_q)$, $h(y) = 1/\sigma(1 + \xi y/\sigma)^{-1/\xi-1}$ is the density of the generalized Pareto distribution, and $g_{\kappa(\mathbf{x})} = dG_{\kappa(\mathbf{x})}/dy$. In a Bayesian context the Lasso can be interpreted as posterior mode estimates when the regression parameters have independent and identical Laplace priors (i.e. double exponential), that is, $\pi(\beta_j) \propto e^{-\lambda/2|\beta_j|}$; see Tibshirani (1996) and Reich and Ghosh (2019, Section 4.2.3). Following Park and Casella (2008), we assume a Gamma prior on λ^2 . The hierarchical representation of the first version of our Bayesian Lasso conditional EGPD for an heavy tailed response is thus:

Extreme Value Bayesian Lasso for the Conditional Bulk and Tail (1st version)

1. Likelihood

$$y_i \mid \mathbf{x}_i, \boldsymbol{\beta}, \sigma, \xi, \lambda^2 \sim \text{EGPD}_G(\kappa(\mathbf{x}_i), \sigma, \xi), \quad i = 1, \dots, n,$$

$$\kappa(\mathbf{x}) = k(\mathbf{x}^T \boldsymbol{\beta}). \quad (7)$$

2. Priors

$$\begin{cases} \boldsymbol{\beta} \mid \lambda \sim \text{Laplace}(\lambda), \\ \lambda^2 \sim \text{Gamma}(a_\lambda, b_\lambda), \\ \sigma \sim \text{Gamma}(a_\sigma, b_\sigma), \\ \xi \sim \pi_\xi. \end{cases}$$

If the phenomena of interest are a priori heavy-tailed, then it may be sensible to set $\pi_\xi = \text{Gamma}(a_\xi, b_\xi)$, whereas $\pi_\xi = \text{N}(\mu_\xi, \sigma_\xi)$ may be sensible if all domains attraction are equally likely a priori.

Since the posterior has no closed form expression we resort to MCMC (Markov Chain Monte Carlo) methods to sample from the posterior. Indeed, if for example $\pi_\xi = \text{Gamma}(a_\xi, b_\xi)$ distribution, then

$$\begin{aligned} p(\boldsymbol{\beta}, \sigma, \xi \mid \mathbf{y}, \mathbf{X}) &\propto \pi(\boldsymbol{\beta})\pi(\sigma)\pi(\xi)L(\boldsymbol{\beta}, \sigma, \xi) \\ &\propto \sigma^{a_\sigma-1}\xi^{a_\xi-1}\exp\left\{-\frac{\lambda}{2}\sum_{j=1}^p|\beta_j|\right\}L(\boldsymbol{\beta}, \sigma, \xi), \end{aligned}$$

where $\mathbf{y} = (y_1, \dots, y_n)$ and $\mathbf{X} = (\mathbf{x}_1 \cdots \mathbf{x}_n)$, and thus the need to resort to MCMC methods.

A shortcoming of the first version of the model—that will be addressed in the next section—is that it only allows for the effect of covariates on the bulk, but not on the tail; this is a consequence of the fact that only the part of the model that drives the bulk, $\kappa(\mathbf{x})$, is indexed by a covariate.

2.4 EXTENSIONS FOR COVARIATE-ADJUSTED TAIL

In practice some covariates can be significant for the bulk but not for the tail—or the other way around. Thus, we extend the specification from Sections 2.2–2.3, by also allowing parameters underlying the tail to also depend on a covariate. Specifically, we consider the following specification:

$$F(y \mid \mathbf{x}) = G_{\kappa(\mathbf{x})}(H(y \mid \mathbf{x})), \quad (8)$$

where $H(y \mid \mathbf{x})$ is a reparametrized conditional generalized Pareto distribution, with parameters $\nu(\mathbf{x}) = \sigma(\mathbf{x})\{1 + \xi(\mathbf{x})\}$ and $\xi(\mathbf{x})$, that is

$$H(y \mid \mathbf{x}) = 1 - \left[1 + \frac{\xi(\mathbf{x})\{1 + \xi(\mathbf{x})\}y}{\nu(\mathbf{x})}\right]^{-1/\xi}.$$

Here, $\kappa(\mathbf{x})$ is a function as in (7) whereas $\nu(\mathbf{x}) = \ell(\mathbf{x}^T \boldsymbol{\alpha})$ and $\xi(\mathbf{x}) = \mu(\mathbf{x}^T \boldsymbol{\gamma})$, with ℓ and μ being inverse-link functions. The canonical embodiment of the full version of our model is obtained by specifying $G_{\kappa(\mathbf{x})}(v) = v^{\kappa(\mathbf{x})}$ along with

$$\kappa(\mathbf{x}) = \exp(\mathbf{x}^T \boldsymbol{\beta}), \quad \nu(\mathbf{x}) = \exp(\mathbf{x}^T \boldsymbol{\alpha}), \quad \xi(\mathbf{x}) = \exp(\mathbf{x}^T \boldsymbol{\gamma}).$$

The schematic representation below summarizes our model:

Extreme Value Bayesian Lasso for the Conditional Bulk and Tail (2nd version)

1. Likelihood

$$y_i \mid \mathbf{x}_i, \boldsymbol{\alpha}, \boldsymbol{\beta}, \boldsymbol{\gamma}, \lambda_\alpha \sim \text{EGPD}_G(\kappa(\mathbf{x}_i), \sigma(\mathbf{x}_i), \xi(\mathbf{x}_i)), \quad i = 1, \dots, n,$$

$$\kappa(\mathbf{x}) = k(\mathbf{x}^T \boldsymbol{\beta}), \quad \nu(\mathbf{x}) = \ell(\mathbf{x}^T \boldsymbol{\alpha}), \quad \xi(\mathbf{x}) = \mu(\mathbf{x}^T \boldsymbol{\gamma}). \quad (9)$$

2. Priors

$$\begin{cases} \boldsymbol{\beta} \mid \lambda \sim \text{Laplace}(\lambda), \\ \boldsymbol{\alpha} \mid \lambda \sim \text{Laplace}(\lambda), \\ \boldsymbol{\gamma} \mid \lambda \sim \text{Laplace}(\lambda). \\ \lambda \sim \text{Gamma}(a, b), \end{cases}$$

The specification in (8) warrants some remarks:

1. *The need for a reparametrization:* While it would seem natural to simply index (σ, ξ) with a covariate and to proceed as in Sections 2.2–2.3, similarly to Chavez-Demoulin and Davison (2005) and Cabras and Castellanos (2011), who work in a GPD setting we found that approach to be computationally unstable; in particular, in our case the latter parametrization leads to poor mixing and to small effective sample sizes.
2. *Any potential reparametrization should keep parameters for the bulk and tails separated:* Since we aim to learn which covariates are important for the bulk and tail, any reparametrization to be made should not mix the parameters for the conditional bulk and tails, i.e., we look for reparametrizations of the type

$$(\kappa, \sigma, \xi) \mapsto (\kappa, \nu(\sigma, \xi), \xi) \quad \text{or} \quad (\kappa, \sigma, \xi) \mapsto (\kappa, \sigma, \zeta(\sigma, \xi)).$$

3. *Fisher information*: Parameter orthogonality (Young and Smith, 2005, Section 9.2) requires the computation of the Fisher information matrix. Since the canonical EGPD is a particular case of the so-called Generalized Feller–Pareto distribution (Kleiber and Kotz, 2003), with $(a, b, p, q, r) = (1, \sigma/\xi, \kappa, 1, 1/\xi)$, as

$$h_{\text{GFP}}(y) = \frac{ary^{a-1}}{b^a B(p, q)} \left\{ 1 + \left(\frac{y}{b} \right)^a \right\}^{-rq-1} \left[1 - \left\{ 1 + \left(\frac{y}{b} \right)^a \right\}^{-r} \right]^{p-1}, \quad y > 0,$$

where $B(p, q) = \int_0^1 t^{p-1} (1-t)^{q-1} dt$, the entries of the Fisher information matrix follow from Mahmoud and Abd El-Ghafour (2015, Section 3); yet the matrix is rather intricate and thus we decided to look for a more sensible way to proceed than attempting to achieve parameter orthogonality.

The reparametrization $(\sigma, \xi) \mapsto (\sigma(1+\xi), \xi)$ is orthogonal for the case of the GPD for $\xi > -1/2$ (Chavez-Demoulin and Davison, 2005), but it is only approximately orthogonal for the EGPD in a neighborhood of $\kappa = 1$. Heuristically, this can be seen by contrasting the likelihood of the canonical EGPD (l) with that of the GPD (l^*); to streamline the argument, we concentrate on the single observation case (y) but the derivations below hold more generally. The starting point is that

$$l(\boldsymbol{\psi}) = l(\kappa, \boldsymbol{\theta}) = l^*(\boldsymbol{\theta}) + \log \kappa + (\kappa - 1) \log\{H(y)\}, \quad (10)$$

where $\boldsymbol{\psi} = (\kappa, \sigma, \xi)$ and $\boldsymbol{\theta} = (\sigma, \xi)$, and thus it follows from (10) that $l(\boldsymbol{\psi}) \approx l^*(\boldsymbol{\theta})$, in a neighborhood of $\kappa = 1$; a similar relation holds for the corresponding Fisher informations,

$$I_{\psi} = -E_{\psi} \left(\frac{\partial l}{\partial \boldsymbol{\psi} \partial \boldsymbol{\psi}^T} \right) = \begin{pmatrix} I_{\theta} & I_{\theta, \kappa} \\ I_{\kappa, \theta} & I_{\kappa} \end{pmatrix}, \quad I_{\theta}^* = -E_{\theta} \left(\frac{\partial l^*}{\partial \boldsymbol{\theta} \partial \boldsymbol{\theta}^T} \right),$$

where $E_{\theta}(\cdot) = \int \cdot h_{\theta}(y) dy$ and $E_{\psi}(\cdot) = \int \cdot h_{\theta}(y) g(H_{\theta}(y)) dy$. Indeed, it can be shown that

$$I_{\theta} = -E_{\psi} \left(\frac{\partial^2 l^*}{\partial \boldsymbol{\theta}^2} \right) + (\kappa - 1) E_{\psi} \{m(\boldsymbol{\theta})\},$$

where

$$m(\boldsymbol{\theta}) = \left[H(y) \frac{\partial^2 H}{\partial \boldsymbol{\theta}^2}(y) + \left\{ \frac{\partial^2 H}{\partial \boldsymbol{\theta}^2}(y) \right\}^2 \right] / \{H(y)\}^2$$

thus suggesting that $I_{\theta} \approx I_{\theta}^*$ in a neighborhood of $\kappa = 1$. Despite the fact the reparametrization is only quasi-orthogonal for (σ, ξ) in an EGPD framework, the numerical studies reported in Section 3 indicate a very good computational performance.

3 SIMULATION STUDY

3.1 SIMULATION SCENARIOS AND ONE-SHOT EXPERIMENTS

In this section we describe the simulation scenarios and present one-shot experiments so to illustrate the proposed method; a Monte Carlo study will be later presented in Section 3.2. For now, we focus on describing the setting over which we simulate the data and on discussing the numerical experiments; `jags` (Plummer, 2019) code for implementing our methods is available from the Supplementary Material.

Data are simulated according to (8), with power carrier $G_{\kappa(\mathbf{x})}(v) = v^{\kappa(\mathbf{x})}$ and with link functions

$$\kappa_{\mathbf{x}} = \exp(\mathbf{x}^T \boldsymbol{\beta}), \quad \nu_{\mathbf{x}} = \exp(\mathbf{x}^T \boldsymbol{\alpha}), \quad \xi_{\mathbf{x}} = \exp(\mathbf{x}^T \boldsymbol{\gamma}).$$

We consider four scenarios:

- **Scenario 1**—Light effects for bulk, light effects for tail:

$$\begin{cases} \boldsymbol{\beta} = (0.3, 0, 0.3, 0, 0, -0.3, 0, 0, 0, -0.3) \\ \boldsymbol{\alpha} = (0, -0.3, 0, 0, 0.3, 0, 0, 0.3, 0, 0) \\ \boldsymbol{\gamma} = (0.3, 0, 0, 0.3, 0, 0, 0, 0, 0.3, -0.3) \end{cases}$$

- **Scenario 2**—Light effects for bulk, large effects for tail:

$$\begin{cases} \boldsymbol{\beta} = (0.3, 0, 0.3, 0, 0, -0.3, 0, 0, 0, -0.3) \\ \boldsymbol{\alpha} = (0, -0.6, 0, 0, 0.6, 0, 0, 0.6, 0, 0) \\ \boldsymbol{\gamma} = (0.6, 0, 0, 0.6, 0, 0, 0, 0, 0.6, -0.6) \end{cases}$$

- **Scenario 3**—Large effects for bulk, light effects for tail:

$$\begin{cases} \boldsymbol{\beta} = (0.6, 0, 0.6, 0, 0, -0.6, 0, 0, 0, -0.6) \\ \boldsymbol{\alpha} = (0, -0.3, 0, 0, 0.3, 0, 0, 0.3, 0, 0) \\ \boldsymbol{\gamma} = (0.3, 0, 0, 0.3, 0, 0, 0, 0, 0.3, -0.3) \end{cases}$$

- **Scenario 4**—Large effects for bulk, large effects for tail:

$$\begin{cases} \boldsymbol{\beta} = (0.6, 0, 0.6, 0, 0, -0.6, 0, 0, 0, -0.6) \\ \boldsymbol{\alpha} = (0, -0.6, 0, 0, 0.6, 0, 0, 0.6, 0, 0) \\ \boldsymbol{\gamma} = (0.6, 0, 0, 0.6, 0, 0, 0, 0, 0.6, -0.6) \end{cases}$$

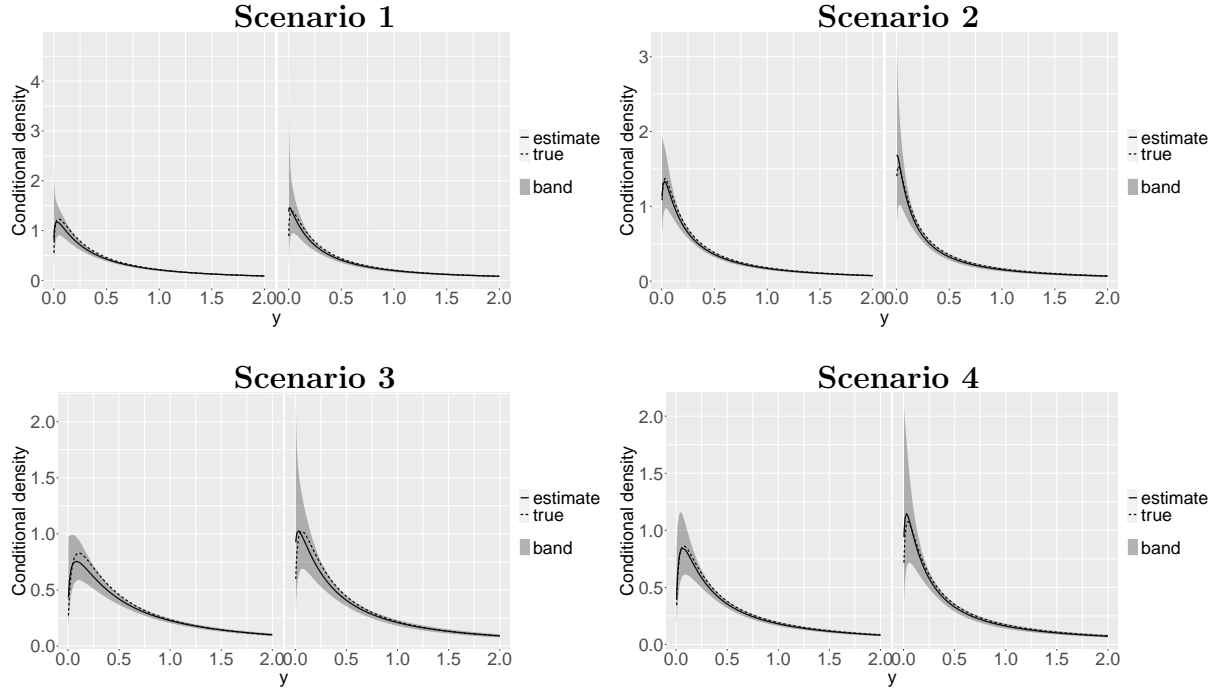


Figure 1: Cross sections of conditional density estimates (solid) along with credible bands against true (dashed) for a one-shot experiment with $n = 500$; the cross sections result from conditioning on $\mathbf{x} = (0.25, \dots, 0.25)$ (left) and $\mathbf{x} = (0.50, \dots, 0.50)$ (right).

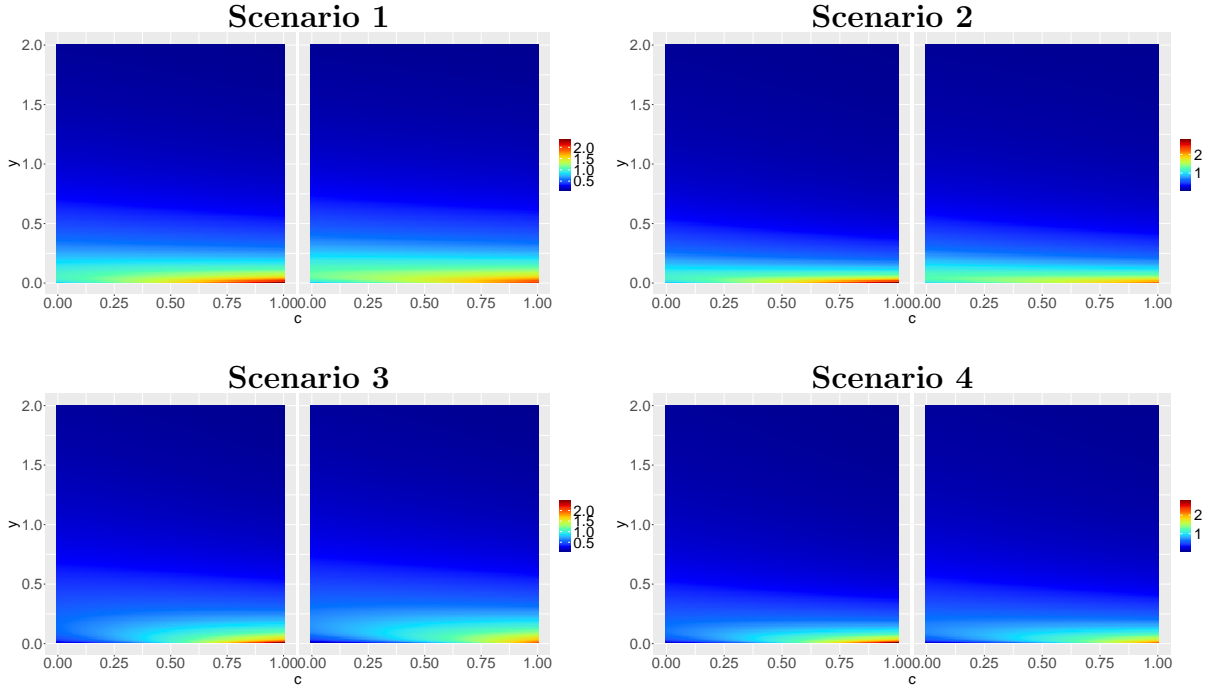


Figure 2: Heatmaps for conditional density estimate for a one-shot experiment with $n = 500$ (left) against those of true conditional density (right).

For each of the scenarios above, we simulate $n = 500$ observations, $\{(\mathbf{x}_i, y_i)\}_{i=1}^n$, from a conditional EGPD with a canonical carrier function; this is about the same number of observations that we analyze in the data application from Section 4. The covariates are simulated from independent standard uniform distributions. Figure 1 shows cross sections of the true and conditional densities for Scenarios 1–4 estimated using our methods, whereas Figure 2 depicts heatmaps obtained by conditioning on $\mathbf{x} = (c, \dots, c)$ with $c \in (0, 1)$. As it can be seen from these figures the method recovers satisfactorily well the true conditional density—especially keeping in mind that only 500 observations are simulated. Of course all these results should be interpreted keeping in mind that they are the outcome of a single-run experiment; Monte Carlo evidence will be presented in the next section.

3.2 MONTE CARLO SIMULATION STUDY

To assess the finite-sample performance of the proposed methods we now present the results of a Monte Carlo simulation study, where we repeat 1 000 times the one-shot experiments from Section 3.1. We consider the following sample sizes, $n = 100$, $n = 250$, and $n = 500$.

We start with the regression coefficient estimates. Figure 3 presents side-by-side boxplots of the coefficient estimates for each scenario for the case $n = 250$. As it can be seen from Figure 3, the estimates tend to be close to the true values thus suggesting that the proposed methods are able to learn what covariates are significant for the bulk, but not for the tail—and vice-versa; further experiments (results not shown) indicate that performance may deteriorate if the number of common effects between tail and bulk is large. The coefficient estimates for the cases $n = 100$ and $n = 500$ are reported in the Supplementary Material, and as expected the larger the sample size the more accurate the estimates.

We now move to the conditional density. To compare the fitted conditional density against the true as the sample size increases, we resort to the Mean Integrated Squared Error (MISE):

$$\text{MISE} = \mathbb{E} \left(\int \int \{ \widehat{f}(y | \mathbf{x}) - f(y | \mathbf{x}) \}^2 d\mathbf{x} dy \right).$$

Figure 4 presents a boxplot with the MISE for each run of the simulation experiment. As it can be seen from Figure 4, MISE tends to decrease as the n increases, thus indicating that a better performance of the proposed methods is to be expected on larger samples.

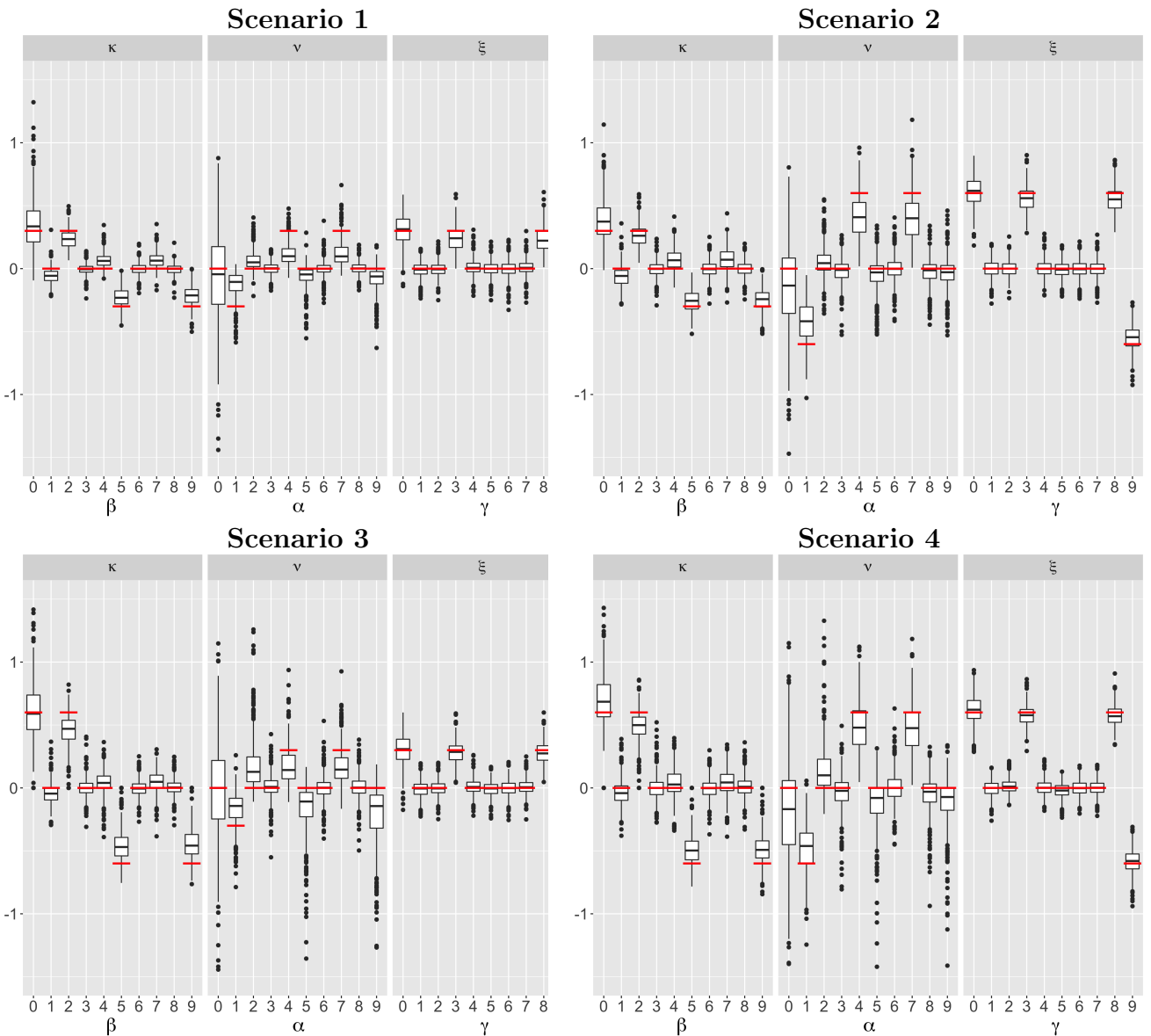


Figure 3: Side-by-side boxplots with regression coefficient estimates for Monte Carlo simulation study ($n = 250$) plotted against the true values (—).

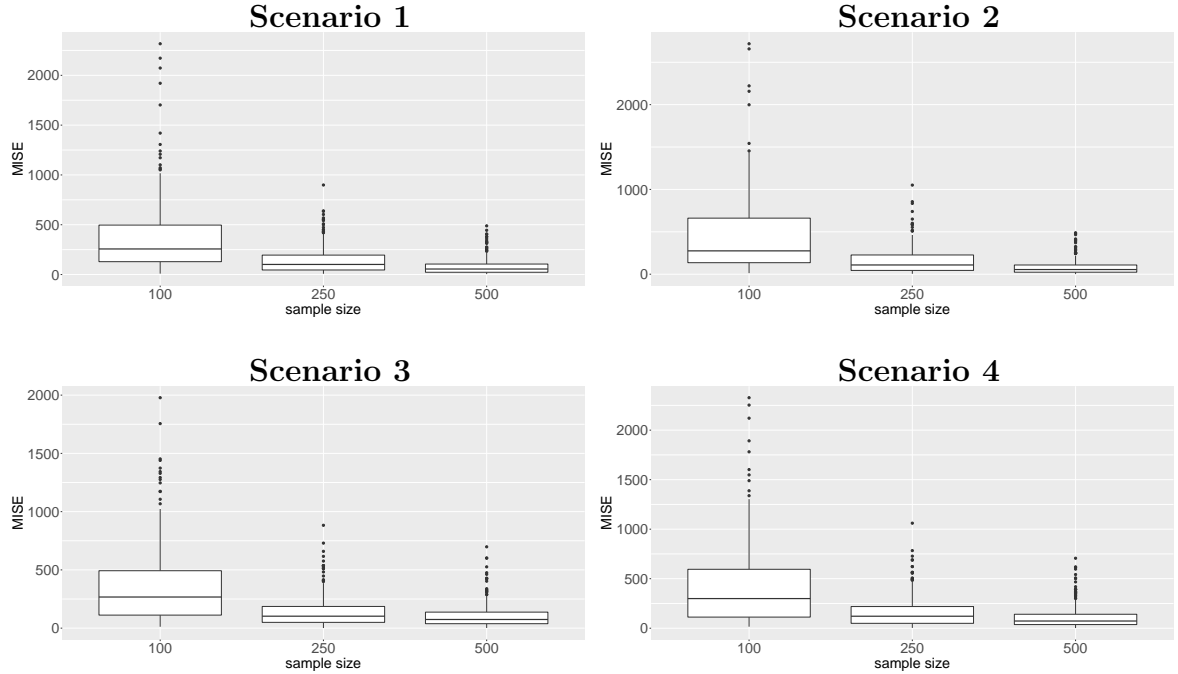


Figure 4: Side-by-side boxplots of MISE for Monte Carlo simulation study.

4 DRIVERS OF MODERATE AND EXTREME RAINFALL IN MADEIRA

4.1 MOTIVATION, APPLIED CONTEXT, AND DATA DESCRIPTION

We now showcase the proposed methodology with a climatological illustration with data from Funchal, Madeira (Portugal); the island of Madeira is an archipelago of volcanic origin located in the Atlantic Ocean, about 900km southwest of mainland Portugal. Prior to fitting the proposed model, we start by providing some background on the scientific problem of interest and by describing the data. Madeira has suffered a variety of extreme rainfall events over the last two centuries, including the flash floods of October 1803 (800–1000 casualties) and those of February 2010—the latter with a death toll of 45 people (Fragoso et al., 2012; Santos et al., 2017) and with an estimated damage of 1.4 billion Euro (Baioni et al., 2011). Such violent rainfall events are often followed by damaging landslides events, including debris, earth, and mud flows.

To analyze such rainfall events in Funchal, Madeira, we have gathered data from the National Oceanic and Atmospheric Administration (www.noaa.gov). Specifically, we have gathered total monthly precipitation (.01 inches), as well as the following potential drivers for extreme rainfall: Atlantic multi-decadal Oscillation (AMO), El Niño-Southern Oscillation (expressed by NINO34

index) (ENSO), North Pacific Index (NP), Pacific Decadal Oscillation (PDO), Southern Oscillation Index (SOI), and North Atlantic Oscillation (NAO). The sample period covers January 1973 to June 2018, thus including episodes such as the violent flash floods of 1979, 1993, 2001, and 2010 (Baioni et al., 2011). After eliminating the dry events (i.e. zero precipitation) and the missing precipitation data (two observations), we are left with a total of 532 observations.

The potential drivers for extreme rainfall above have been widely examined in the climatological literature, mainly on large landmasses. In particular, it has been suggested that in North America ENSO, PDO, and NAO play a key role governing the occurrence of extreme rainfall events (Kenyon and Hegerl, 2010; Zhang et al., 2010; Whan and Zwiers, 2017); yet for the UK, while NAO is believed to impact the occurrence of extreme rainfall events, no influence of PDO nor AMO has been detected (Brown, 2018). The many peculiarities surrounding Madeira climate (e.g. Azores anticyclone, Canary current, Gulf stream, *etc*), along with the negative impact that flash floods and landslide events produce on the island, motivate us to ask: i) whether such drivers are relevant for explaining extreme rainfall episodes in Madeira; ii) whether such drivers are also relevant for moderate rainfall events.

4.2 TRACKING DRIVERS OF MODERATE AND EXTREME RAINFALL

One of the goals of the analysis is to use the lenses of our model so to learn what are the drivers of moderate and extreme rainfall in Funchal. To conduct such inquiry, we use the full model from Section 2.4 (see Eq. (9)), with power carrier $G_{\kappa(\mathbf{x})}(v) = v^{\kappa(\mathbf{x})}$ and with link functions

$$\kappa(\mathbf{x}) = \exp(\mathbf{x}^T \boldsymbol{\beta}), \quad \nu(\mathbf{x}) = \exp(\mathbf{x}^T \boldsymbol{\alpha}), \quad \xi(\mathbf{x}) = \mathbf{x}^T \boldsymbol{\gamma}.$$

Covariates have been standardized, and we used a flat Normal prior, $N(0, 100^2)$, for the intercepts, and an uninformative Gamma prior, $\text{Gamma}(0.1, 0.1)$, for the hyperparameter λ . After a burn-in period of 1 000 iterations, we collected a total of 20 000 posterior samples. The results of MCMC convergence diagnostics were satisfactory; in particular, the effective sample sizes are acceptably high, ranging from about 1 300 to 5 700, and all values of Geweke's diagnostic are satisfactory, ranging from about -0.8 to 1.5. Figure 5 depicts the credible bands for each regression coefficient. To assess the fit of the proposed model we resort to randomized quantile residuals (Dunn and Smyth, 1996). Figure 6 depicts the corresponding randomized quantile

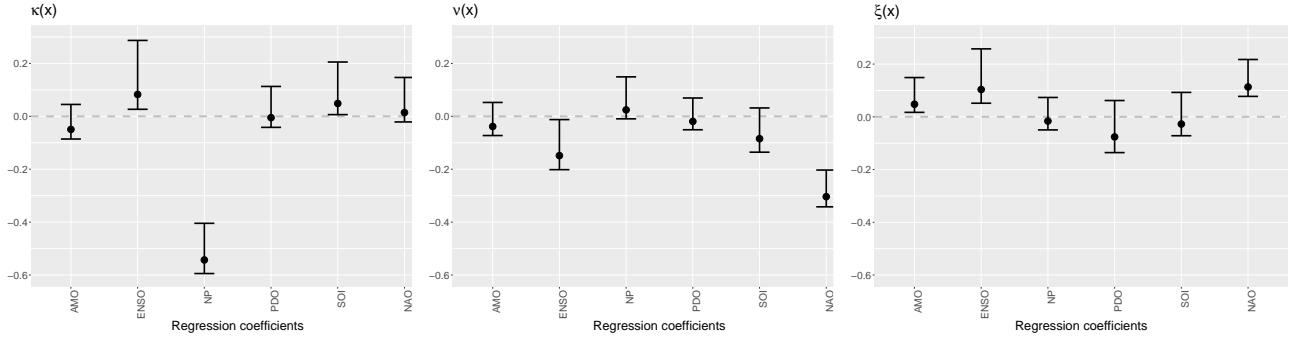


Figure 5: Credible bands for regression coefficients for inverse-link functions; the dots (\bullet) represent the posterior means and the dashed line represents the reference line $\beta = 0$.

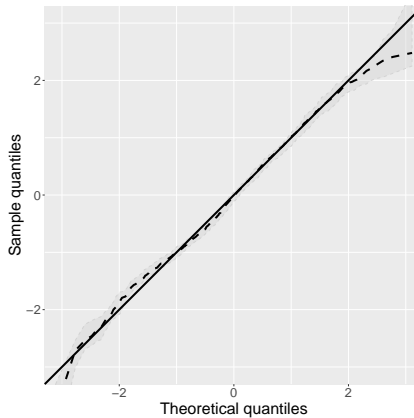


Figure 6: Randomized quantile residuals; the dashed line represents the posterior mean plotted along with credible bands.

residuals against the theoretical standard normal quantiles, and it evidences an acceptably good fit of the model.

As it can be seen from Figure 5 (middle and right), the proposed methods suggest that the key drivers for extreme rainfall in Funchal are NAO and ENSO, along with a possible modest influence of AMO on the magnitude of extreme rainfall events. To put it differently, such results hint that a higher NAO, ENSO, and AMO tend to be associated with extreme rainfall episodes in Funchal. Such findings are thus reasonably in line with those of Kenyon and Hegerl (2010) Zhang et al. (2010), and Whan and Zwiers (2017) for North America. Yet, similarly to Brown (2018), we find no relevant impact of PDO on extreme rainfall spells. Interestingly, of all these potential drivers for extreme rainfall, only one (ENSO) seems to be statistically associated with moderate rainfall; see Figure 5 (left). Also, NP is the most relevant driver of moderate rainfall, and yet the analysis suggests it plays no role on extreme rainfall. Additionally, Figure 5 (left) suggests that an increase in NP leads to an heavier left tail (i.e. dryer months), whereas an

increase in ENSO leads to less mass close to zero (i.e. rainy months).

5 CLOSING REMARKS

In this paper we have introduced a Lasso-type model for the bulk and tail of a possibly heavy-tailed response. The proposed model: i) bypasses the need for threshold selection (u_x); ii) models both the conditional bulk and conditional tails; iii) it is naturally tailored for variable selection. Interestingly, the model can be regarded as a Lasso-type model for quantile regression that is tailored for both the bulk and for extrapolating into the tails. As a byproduct, our paper has some points of contact with the Bayesian literature on Bayesian distributional regression (Umlauf and Kneib, 2018), and it has links with the recent paper Groll et al. (2019).

Some final comments on future research are in order. A version of our model that includes additionally a regression model for point masses at zero would be natural for a variety of contexts, such as for modeling long periods without rain or droughts. Semicontinuous responses that consist of a mixture of 0's and a continuous positive distribution are indeed common in practice (e.g. Olsen and Schafer, 2001). Another natural avenue for future research would endow the model with further flexibility by resorting to a generalized additive model, where the smooth function of each covariate is modeled using B-spline basis functions. The latter extension would however require a group lasso (Yuan and Lin, 2006), shrinking groups of regression coefficients (per smooth function) towards zero. While here we focus on modeling positive random variables, another interesting extension of the proposed model would consider the left end-point itself as a parameter—rather than fixing it at zero. Finally, from an inference perspective it would also seem natural defining a semiparametric Bayesian version of our model that would set a prior directly on the covariate-specific carrier function $G_{\mathbf{x}}$ —rather than specifying a power carrier function in advance—and to model the conditional density as $F(y | \mathbf{x}) = G_{\mathbf{x}}(H(y | \mathbf{x}))$. This approach would however require setting a prior on the space \mathcal{G} of all carrier functions so to ensure that $G_{\mathbf{x}}$ obeys Assumptions A, B and C, for all \mathbf{x} . While priors on spaces of functions are an active field of research (Ghosal and Van der Vaart, 2015), definition of priors over \mathcal{G} is to our knowledge an open problem; a natural line of attack to construct such a prior would be via random Bernstein polynomials (Petrone and Wasserman, 2002), with weight constraints derived from Lemma 1 of Tencaliec et al. (2019).

ACKNOWLEDGMENTS

We thank participants of IWSM (International Workshop on Statistical Modeling) 2019 and of EVA 2019 for constructive comments and discussions. We also thank, without implicating, Vanda Inácio, Ioannis Papastathopoulos, Philippe Naveau, Antónia Turkman, and Feridun Turkman for helpful comments and fruitful discussions. This work was partially supported by FCT (Fundação para a Ciência e a Tecnologia, Portugal), through the projects PTDC/MAT-STA/28649/2017 and UID/MAT/00006/2020.

References

Arnold, B. C. and Press, S. J. (1989), Bayesian estimation and prediction for Pareto data, *Journal of the American Statistical Association*, 84, 1079–1084.

Baioni, D., Castaldini, D., and Cencetti, C. (2011), Human activity and damaging landslides and floods on Madeira Island. *Natural Hazards & Earth System Sciences*, 11, 3035–3046.

Behrens, C. N., Lopes, H. F., and Gamerman, D. (2004), Bayesian analysis of extreme events with threshold estimation, *Statistical Modelling*, 4, 227–244.

Beirlant, J., Goegebeur, Y., Segers, J., and Teugels, J. (2004), *Statistics of Extremes: Theory and Applications*, Wiley, Hoboken, NJ: Wiley.

Brown, S. J. (2018), The drivers of variability in UK extreme rainfall, *International Journal of Climatology*, 38, e119–e130.

Cabras, S. and Castellanos, M. E. (2011), A Bayesian approach for estimating extreme quantiles under a semiparametric mixture model, *ASTIN Bulletin*, 41, 87–106.

Carreau, J. and Bengio, Y. (2009), A hybrid Pareto model for asymmetric fat-tailed data: The univariate case, *Extremes*, 12, 53–76.

Castellanos, M. E. and Cabras, S. (2007), A default Bayesian procedure for the generalized Pareto distribution, *Journal of Statistical Planning and Inference*, 137, 473–483.

Chavez-Demoulin, V. and Davison, A. C. (2005), Generalized additive modelling of sample extremes, *Journal of the Royal Statistical Society: Series C (Applied Statistics)*, 54, 207–222.

Chavez-Demoulin, V., Embrechts, P., and Hofert, M. (2016), An extreme value approach for modeling operational risk losses depending on covariates, *Journal of Risk and Insurance*, 83, 735–776.

Chernozhukov, V. (2005), Extremal quantile regression, *Annals of Statistics*, 33, 806–839.

Coles, S. (2001), *An Introduction to Statistical Modeling of Extreme Values*, London: Springer.

Davison, A. C. and Smith, R. L. (1990), Models for exceedances over high thresholds, *Journal of the Royal Statistical Society: Series B (Methodological)*, 393–442.

de Zea Bermudez, P. and Kotz, S. (2010), Parameter estimation of the generalized Pareto distribution—Part II, *Journal of Statistical Planning and Inference*, 140, 1374–1388.

de Zea Bermudez, P. and Turkman, M. A. (2003), Bayesian approach to parameter estimation of the generalized

Pareto distribution, *Test*, 12, 259–277.

do Nascimento, F. F., Gamerman, D., and Lopes, H. F. (2012), A semiparametric Bayesian approach to extreme value estimation, *Statistics and Computing*, 22, 661–675.

Dunn, P. K. and Smyth, G. K. (1996), Randomized quantile residuals, *Journal of Computational and Graphical Statistics*, 5, 236–244.

Eastoe, E. F. and Tawn, J. A. (2009), Modelling non-stationary extremes with application to surface level ozone, *Journal of the Royal Statistical Society: Series C (Applied Statistics)*, 58, 25–45.

Embrechts, P., Klüppelberg, C., and Mikosch, T. (1997), *Modelling Extremal Events for Insurance and Finance*, New York: Springer.

Fragoso, M., Trigo, R., Pinto, J., Lopes, S., Lopes, A., Ulbrich, S., and Magro, C. (2012), The 20 February 2010 Madeira flash-floods: synoptic analysis and extreme rainfall assessment, *Natural Hazards and Earth System Sciences*, 12, 715–730.

Frigessi, A., Haug, O., and Rue, H. (2002), A dynamic mixture model for unsupervised tail estimation without threshold selection, *Extremes*, 5, 219–235.

Ghosal, S. and Van der Vaart, A. W. (2015), *Fundamentals of Nonparametric Bayesian Inference*, Cambridge University Press, Cambridge.

Groll, A., Hambuckers, J., Kneib, T., and Umlauf, N. (2019), LASSO-type penalization in the framework of generalized additive models for location, scale and shape, *Computational Statistics & Data Analysis*, 140, 59–73.

Huser, R. and Genton, M. G. (2016), Non-stationary dependence structures for spatial extremes, *Journal of Agricultural, Biological, and Environmental Statistics*, 21, 470–491.

Kenyon, J. and Hegerl, G. C. (2010), Influence of modes of climate variability on global precipitation extremes, *Journal of Climate*, 23, 6248–6262.

Kleiber, C. and Kotz, S. (2003), *Statistical Size Distributions in Economics and Actuarial Sciences*, New York: Wiley.

Koenker, R. (2005), *Quantile Regression*, Cambridge, MA: Cambridge University Press.

Koenker, R. and Bassett, G. (1978), Regression quantiles, *Econometrica*, 33–50.

MacDonald, A., Scarrott, C., Lee, D., Darlow, B., Reale, M., and Russell, G. (2011), A flexible extreme value mixture model, *Computational Statistics & Data Analysis*, 55, 2137–2157.

Mahmoud, M. R. and Abd El-Ghafour, A. S. (2015), Fisher information matrix for the generalized Feller–Pareto distribution, *Communications in Statistics—Theory and Methods*, 44, 4396–4407.

Naveau, P., Huser, R., Ribereau, P., and Hannart, A. (2016), Modeling jointly low, moderate, and heavy rainfall intensities without a threshold selection, *Water Resources Research*, 52, 2753–2769.

Olsen, M. K. and Schafer, J. L. (2001), A two-part random-effects model for semicontinuous longitudinal data, *Journal of the American Statistical Association*, 96, 730–745.

Papastathopoulos, I. and Tawn, J. A. (2013), Extended generalised Pareto models for tail estimation, *Journal of Statistical Planning and Inference*, 143, 131–143.

Park, T. and Casella, G. (2008), The Bayesian lasso, *Journal of the American Statistical Association*, 103, 681–686.

Petrone, S. and Wasserman, L. (2002), Consistency of Bernstein polynomial posteriors, *Journal of the Royal Statistical Society: Series B (Statistical Methodology)*, 64, 79–100.

Plummer, M. (2019), rjags: Bayesian graphical models using MCMC. R package version 4-10, URL <http://CRAN.R-project.org/package=rjags>.

Polson, N. G. and Sokolov, V. (2019), Bayesian regularization: From Tikhonov to horseshoe, *Wiley Interdisciplinary Reviews: Computational Statistics*, e1463.

Reich, B. J. and Ghosh, S. K. (2019), *Bayesian Statistical Methods*, Boca Raton, FL: Chapman & Hall/CRC.

Resnick, S. I. (1971), Tail equivalence and its applications, *Journal of Applied Probability*, 8, 136–156.

Santos, M., Santos, J. A., and Fragoso, M. (2017), Atmospheric driving mechanisms of flash floods in Portugal, *International Journal of Climatology*, 37, 671–680.

Tencaliec, P., Favre, A.-C., Naveau, P., Prieur, C., and Nicolet, G. (2019), Flexible semiparametric Generalized Pareto modeling of the entire range of rainfall amount, *Environmetrics*, e2582.

Tibshirani, R. (1996), Regression shrinkage and selection via the lasso, *Journal of the Royal Statistical Society: Series B*, 58, 267–288.

Umlauf, N. and Kneib, T. (2018), A primer on Bayesian distributional regression, *Statistical Modelling*, 18, 219–247.

Villa, C. (2017), Bayesian estimation of the threshold of a generalised pareto distribution for heavy-tailed observations, *Test*, 26, 95–118.

Wang, H. and Tsai, C.-L. (2009), Tail index regression, *Journal of the American Statistical Association*, 104, 1233–1240.

Whan, K. and Zwiers, F. (2017), The impact of ENSO and the NAO on extreme winter precipitation in North America in observations and regional climate models, *Climate Dynamics*, 48, 1401–1411.

Young, G. A. and Smith, R. L. (2005), *Essentials of Statistical Inference*, Cambridge, UK: Cambridge University Press.

Yuan, M. and Lin, Y. (2006), Model selection and estimation in regression with grouped variables, *Journal of the Royal Statistical Society: Series B*, 68, 49–67.

Zhang, X., Wang, J., Zwiers, F. W., and Groisman, P. Y. (2010), The influence of large-scale climate variability on winter maximum daily precipitation over North America, *Journal of Climate*, 23, 2902–2915.